Surface & Coatings Technology 207 (2012) 50–65

Contents lists available at SciVerse ScienceDirect

Surface & Coatings Technology

journal homepage: www.elsevier.com/locate/surfcoat

Hard nanocomposite coatings: Thermal stability, oxidation resistance and toughness

J. Musil

Department of Physics, Faculty of Applied Sciences, University of West Bohemia, Univerzitní 22, CZ-30614 Plzeň, Czech Republic

ARTICLE INFO

Article history:
Received 16 December 2011
Accepted in revised form 19 May 2012
Available online 26 May 2012

Keywords:
Nanocomposite coatings
Hardness and toughness
Thermal stability
Resistance to oxidation
Resistance to cracking
Magnetron sputtering

ABSTRACT

The article reports on the enhanced hardness of nanocomposite coatings, their thermal stability, protection of the substrate against oxidation at temperatures above 1000 °C, X-ray amorphous coatings thermally stable above 1000 °C and new advanced hard nanocomposite coatings with enhanced toughness which exhibit (i) low values of the effective Young's modulus E^* satisfying the condition $H/E^* > 0.1$, (ii) high elastic recovery $W_e \geq 60\%$, (iii) strongly improved tribological properties, and (iv) enhanced resistance to cracking; here $E^* = E(1-\nu^2)$, E is the Young's modulus and ν is the Poison's ratio. At the end trends of next development of hard nanocomposite coatings are briefly outlined.

1. Introduction

Nanocomposite coatings represent a new generation of materials [1–37]. They are composed of at least two separated phases with nanocrystalline (nc-) and/or amorphous (a-) structure or their combination. The nanocomposite materials, due to very small ($\leq$10 nm) grains and a significant role of boundary regions surrounding individual grains, exhibit enhanced or even completely new properties, and behave in a strongly different manner compared to the conventional materials composed of larger ($\geq$100 nm) grains. These facts are a main driving force stimulating the development of nanocomposite coatings. This article reports on hard nanocomposite coatings and their unique properties.

The main feature of these nanocomposites is an enhanced hardness. The enhanced hardness of the nanocomposite coating H_n can be more than two times greater than that of its harder component. Main mechanisms, which are responsible for the hardness enhancement, are: (1) the dislocation-induced plastic deformation, (2) the nanostructure of materials, and (3) cohesive forces between atoms. The dislocation-induced plastic deformation dominates in the materials composed of large grains with size $d > 10$ nm. On the contrary, the nanostructure is dominant in materials composed of small grains with size $d \leq 10$ nm. It means that the hardness enhancement of coating strongly depends on the grain size d, see Fig. 1. From this figure it is seen that there is a critical value of the grain size $d_c \approx 10$ nm at which a maximum value of hardness H_{max} of the coating is achieved. The regions of d around H_{max}, achieved at $d = d_c$, corresponds to a continuous transition from the activity of *the intragranular processes* at $d > d_c$, dominated by the dislocations and described by the Hall–Petch law ($H \sim D^{-1/2}$) [38,39], to the activity of *the intergranular processes* at $d < d_c$ dominated by the interactions between atoms of neighboring grains and/or by the small-scale sliding in grain boundaries. In materials with the grain size $d \leq d_c$ (1) dislocations are not generated (grain size d is smaller than the length of dislocation) and (2) processes in grain boundary regions play a dominant role over those inside grains. Therefore, besides chemical and electronic bonding between atoms the nanostructure of material plays a dominant role when $d \leq d_c$. It was found that there are at least four types of nanostructures that result in the enhanced hardness of nanocomposite coatings: (1) bilayers with nanosize period λ, (2) the columnar nanostructure, (3) nanograins surrounded by very thin (~1 to 2 ML) tissue phase and (4) the mixture of nanograins with different crystallographic orientations and/or different phases, see Fig. 2; here $\lambda = h_1 + h_2$, h_1 and h_2 is the thickness of first and second layer of the bilayer, respectively, and ML denotes the monolayer.

Individual nanostructures are formed under different conditions using either a sequential deposition of individual layers in the nanosize bilayers or in *transition regions* where the coating structure changes from crystalline through nanocrystalline to amorphous. There are three transition regions: (1) the transition from the crystalline to the X-ray amorphous material, (2) the transition between two crystalline phases of different materials and (3) the transition between two crystallographic orientations of grains of the same material. These regions are schematically displayed in Fig. 3. From this figure is seen that to every transition region

E-mail address: musil@kfy.zcu.cz.

0257-8972/$ – see front matter © 2012 Elsevier B.V. All rights reserved.
doi:10.1016/j.surfcoat.2012.05.073

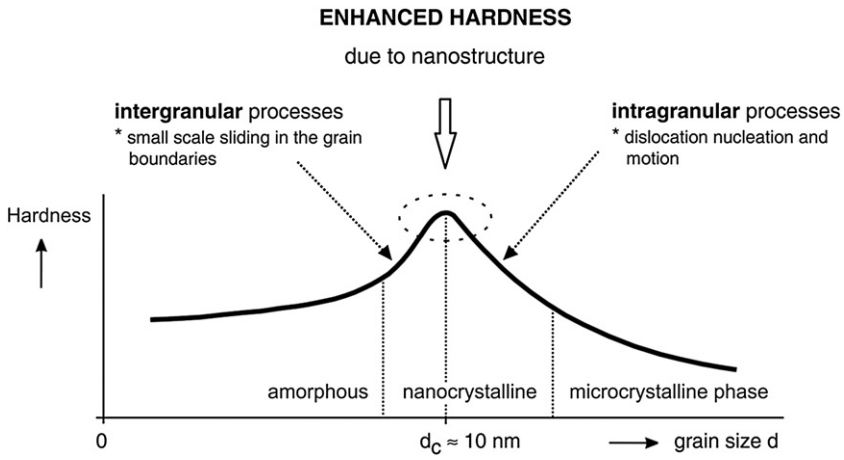

Fig. 1. Schematic illustration of coating hardness as a function of the size d of grains. Adapted after Ref. [27].

corresponds an optimal elemental composition at which nc-/a- or nc-/nc- nanocomposite coatings can be formed. The addition of one or more selected elements into a base material, e.g. the addition of Silicone Si in the nitride transition metal (TM), is very effective way to produce hard nanocomposite coatings with enhanced hardness, here TM = Ti, Zr, Hf, V, Nb, Ta, etc. More details are given in the Refs. [23,27,28].

The energy delivered to the growing film has also a crucial effect on its structure, elemental and phase composition, and physical properties [40–43]. The energy can be delivered by (i) substrate heating E_s, (ii) conversion of the kinetic energy of bombarding ions (E_{bi}) and fast neutrals (E_{fn}) incident on the surface of growing film, i.e. by $E_p = E_{bi} + E_{fn}$, (iii) the heat evolved during formation of the compound E_{ch} (energy released in exothermic chemical reactions), (iv) heating from the sputtered magnetron target E_{mt} which is always not perfectly cooled, and (v) heat radiation from plasma E_{rad}. The total energy E_T delivered to the growing film can be expressed by the following formula [43]

$$E_T = E_s(T_s, t_d) + E_p(U_s, i_s, a_D, p_T, t_d) + E_{ch}(T_s, t_d) + E_{mt}(W_d, t_d, d_{s-t}) + E_{rad}(t_d) \quad (1)$$

where, T_s is the substrate temperature, t_d is the time of film deposition, $p_T = p_{Ar} + p_{RG}$ is the total pressure of sputtering gas mixture, p_{Ar} and p_{RG} are the partial pressure of argon and reactive gas (RG), respectively, $W_d = U_d I_d / S$ is the magnetron target power density, I_d and U_d are the magnetron current and voltage, respectively, S is the whole area of magnetron target and d_{s-t} is the substrate-to-target distance.

In the simplest case of a collisionless, fully ionized plasma in which the component $E_{fn} = 0$ the energy E_p can be expressed in the following form

$$E_p\left[J/cm^3\right] = E_{bi} \approx (U_s i_s)/a_D. \quad (2)$$

Eq. (2) clearly shows two important facts:

1. The energy E_{bi} delivered to the growing film by bombarding ions can be easily calculated from measured deposition parameters (U_s, i_s) and the film deposition rate $a_D = h/t_d$ calculated from measured film thickness h and deposition time t_d.
2. The energy E_{bi} strongly depends not only on U_s and i_s but also on a_D. This fact is of extraordinary importance, particularly in (i) reactive sputtering of compounds and (ii) high-rate sputtering of films. The energy E_{bi} decreases with increasing a_D.

In the case of a higher sputtering pressure p_T, the energy E_{bi} is lower than that defined by Eq. (2) in consequence of collisions between particles and has to be determined from Eq. (3)

$$E_{bi}\left[J/cm^3\right] \approx (U_s i_s) \exp(-L/\lambda_i)/a_D \quad (3)$$

where L is the thickness of voltage sheath and λ_i is the ion mean free path for collisions leading to losses of the ion energy in the sheath. The ion mean free path can be calculated from the Dalton law as λ_i [cm] $\approx 0.4/p_T$ [Pa] [44]. The high-voltage ($U_s \gg U_{fl}$) sheath can be calculated from the Child–Langmuir equation for the dc sheath; here U_{fl}

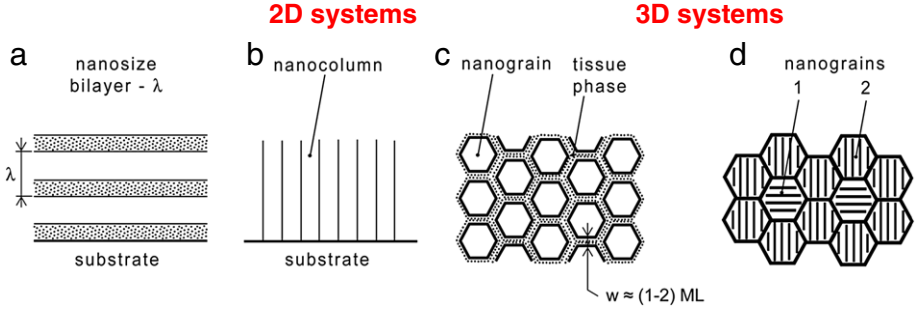

Fig. 2. Schematic illustration of four nanostructures of the nanocomposite coating with enhanced hardness: (a) nanosize bilayers, (b) columnar nanostructure, (c) nanograins surrounded by a tissue phase and (d) mixture of nanograins with different crystallographic orientation.
Adapted after Ref. [28].